AGU PUBLICATIONS

Geophysical Research Letters

RESEARCH LETTER

10.1002/2017GL074455

Key Points:

- We identified 38 slow slip events in southwest Ryukyu using 20 years of continuous GNSS data
- We found that significant increase of the slip accumulation rate of the SSEs occurred twice around 2002 and 2013
- We found that earthquake swarms occurred at the Okinawa Trough in 2002 and 2013 when the SSE slip accumulation accelerated

Supporting Information:

- Supporting Information S1

Correspondence to:
Y. Tu,
yokoemma.jp@gmail.com

Citation:
Tu, Y., & Heki, K. (2017). Decadal modulation of repeating slow slip event activity in the southwestern Ryukyu Arc possibly driven by rifting episodes at the Okinawa Trough. *Geophysical Research Letter*, *44*. https://doi.org/10.1002/2017GL074455

Received 6 JUN 2017
Accepted 6 SEP 2017
Accepted article online 11 SEP 2017

Decadal Modulation of Repeating Slow Slip Event Activity in the Southwestern Ryukyu Arc Possibly Driven by Rifting Episodes at the Okinawa Trough

Yoko Tu[1] and Kosuke Heki[1]

[1]Department Natural History Sciences, Hokkaido University, Sapporo, Japan

Abstract We studied 38 slow slip events (SSEs) in 1997–2016 beneath the Iriomote Island, southwestern Ryukyu Arc, Japan, using continuous Global Navigation Satellite Systems data. These SSEs occur biannually on the same fault patch at a depth of ~30 km on the subducting Philippine Sea Plate slab with average moment magnitudes (M_w) of ~6.6. Here we show that the slip accumulation rate (cumulative slip/lapse time) of these SSEs fluctuated over a decadal time scale. The rate increased twice around 2002 and 2013 concurrently with earthquake swarms in the Okinawa Trough. This suggests that episodic activations of the back-arc spreading at the Okinawa Trough caused extra southward movement of the block south of the trough and accelerated convergence at the Ryukyu Trench.

1. Introduction

Slow slip events (SSEs) are a type of slow earthquakes (Beroza & Ide, 2011) and last from days to weeks (short-term SSEs) or from months to years (long-term SSEs) (Obara & Kato, 2016). Because their fault slips are too slow to generate seismic waves, these events can only be detected by geodetic observations such as Global Navigation Satellite Systems (GNSS) and tiltmeters. SSEs have been observed in several subduction zones around the Pacific Ocean, such as the Nankai Trough, Southwest Japan (Ozawa, 2017), the Boso area, Central Japan (Ozawa, 2014), the Cascadia subduction zone, western Canada (Rogers & Dragert, 2003; Szeliga et al., 2008), Mexico (Vergnolle et al., 2010), and New Zealand (Wallace et al., 2016). SSEs may have mechanical links to large interplate earthquakes in these subduction zones, and it is important to understand their connections. (Obara & Kato, 2016).

The Ryukyu Trench differs from these subduction zones; it is a weakly coupled subduction zone (Uyeda & Kanamori, 1979), and few interplate earthquakes with M_w 8 or more occur there (Ando et al., 2009; Scholz & Campos, 2012). Active back-arc spreading in the Okinawa Trough makes the Ryukyu Arc move trenchward as seen in the GNSS data (Figure 1a), and this makes the fast convergence at the Ryukyu Trench of ~12.5 cm/yr (Heki & Kataoka, 2008).

Recently, Nishimura (2014) identified ~130 short-term SSEs along the entire Ryukyu subduction zone using a detection technique based on Akaike's Information Criterion (AIC). The SSEs repeating beneath the Iriomote Island, in the westernmost part of the Ryukyu Arc, recur approximately twice per year on the same fault patch. They have been studied in detail by Heki and Kataoka (2008), and we study them again using more accurate coordinate data with twice as long a time span as in the previous study, focusing on the time-variable behavior of their slip accumulation rate.

2. Data and Methods

We analyzed GNSS data obtained from 1997 to 2016 at six stations (Figure 1b) of the GNSS Earth Observation Network System (GEONET) operated by the Geospatial Information Authority (GSI) of Japan. We analyzed their daily coordinates using the F3 solution (Nakagawa et al., 2009), and selected the Miyako station as the reference site because this station moves little by the repeating SSEs we study, or by regular earthquakes that occurred in the neighborhood during the studied period (Heki & Kataoka, 2008). We can monitor the SSE signatures with the largest signal-to-noise ratio in the N20W component of the Hateruma station movement (Heki & Kataoka, 2008) (Figure 2a).

Offsets generated by antenna changes were removed in advance, and coseismic jumps by nearby earthquakes were marked with dashed lines (see Figures 2a and 2b). We detected 38 SSEs by visual inspection

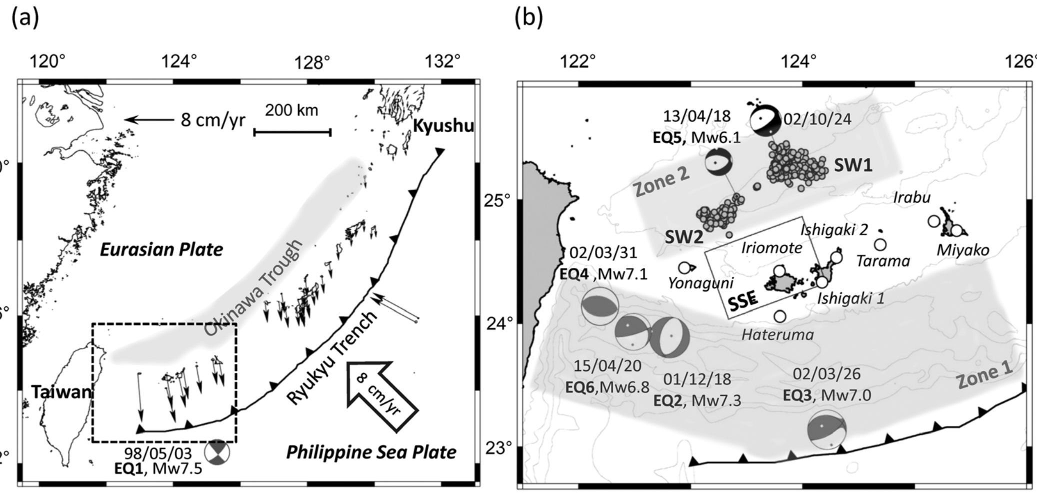

Figure 1. (a) Plate tectonic map of the Ryukyu area. The Philippine Sea Plate subducts beneath the Eurasian Plate along the Ryukyu Trench with a high convergence rate (Heki & Kataoka, 2008). The Okinawa Trough is an active back-arc spreading system, which causes the Ryukyu Arc to move trenchward as demonstrated by the fast southward movement of the GNSS stations. The arrows represent velocities of GNSS stations relative to the Eurasian Plate for the period of 2000–2010. (b) Distribution of the slow slip events (SSEs) (rectangle shows the fault patch), earthquake swarms (gray circles), and six large earthquakes (EQ1–EQ6; EQ1 is shown in Figure 1a). Gray beach balls show the locations and focal mechanisms of large earthquakes along the Ryukyu Trench (EQ1–EQ4 and EQ6). Black beach balls display the source mechanisms of two earthquake swarms (SW1 and SW2 including EQ5) in the Okinawa trough. The gray polygons (zone 1–2) show the geometric extents of earthquakes illustrated in the Figures 4a and 4b. Open circles here depict GEONET GNSS stations used in this study.

with assistance from $-\Delta$AIC, an index showing statistical significance of the SSE onset signatures (Figure 2c) (Nishimura, 2014).

To determine displacement vectors associated with the SSEs, we adopt the same model as Heki and Kataoka (2008) for changes of coordinate x in time t:

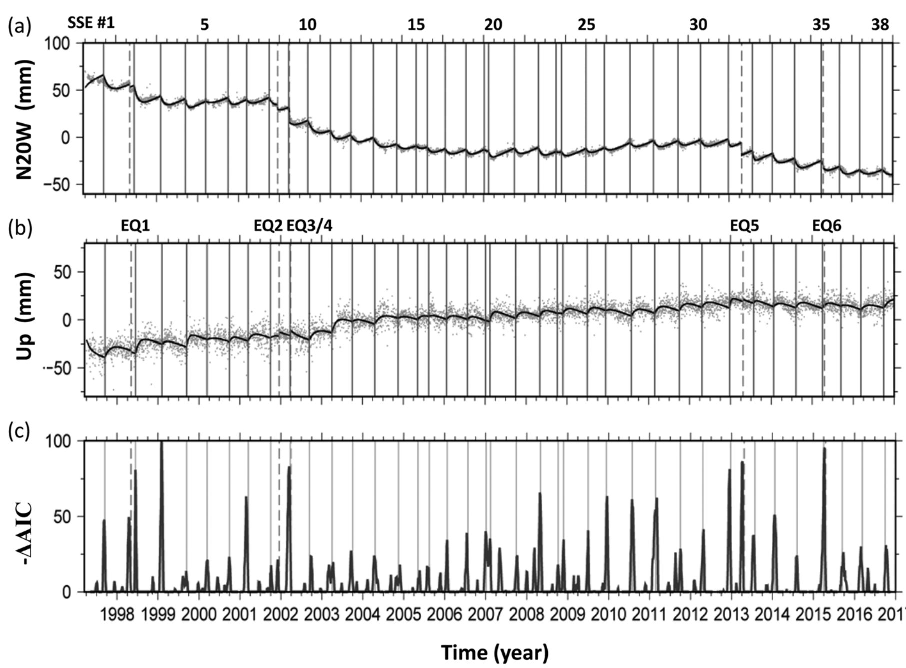

Figure 2. The daily displacements (gray circles) of the Hateruma station relative to Miyako in the (a) N20W and (b) up directions. Solid vertical lines show the onset times of the 38 SSEs; their numbers are marked at the top. Dashed vertical lines indicate six large earthquakes (EQ1–EQ6) during the studied period. Locations and focal mechanisms of these earthquakes are shown in Figures 1a and 1b. (c) The $-\Delta$AIC indicates the significance of the trend change (bending) of the N20W component, or the onset of SSEs (Nishimura, 2014).

$$x = at + b + \sum_{i=1}^{n} X_i \left[1 - \exp\frac{-(t - T_i)}{\tau_i}\right] \quad (T_1 < T_2 < \ldots < T_n < t)$$

where a is the long-term background trend and b is the offset. The number of SSEs before the time t is n, and X_i, T_i, and τ_i are the final displacement, the onset time, and the time constant of the ith SSE, respectively. Three-dimensional (EW, NS, and UD) displacement vectors were used here, while the values of T_i and τ_i were determined by minimizing the postfit residual in the Hateruma N20W time series.

After estimating the three-component displacement vectors at six GNSS stations in all the SSEs, we estimated the slips of the fault patch assuming homogeneous elastic half-space (Okada, 1992). Because of the similar displacement vectors of SSEs, we assumed the same geometry of the fault patch as in Heki and Kataoka (2008), which was confirmed to have the smallest postfit residuals of the displacement vectors. Two components (dip slip and strike slip) of the dislocation vectors were estimated through the least squares method, and the detailed source parameters of these SSEs are given in Table S1 in the supporting information.

3. Results

These 38 SSEs 1997–2016 occurred regularly with an average interval of ~6 months (Figure S1a). Their properties are consistent with Heki and Kataoka (2008), for example, occurrences of these events are not seasonal (Figure S1b), and the average M_w is 6.7. Their time constants (τ_i in the equation) of 0.10–0.15 year lie around the boundary between the short- and long-term SSEs as defined by Obara and Kato (2016). Figure S2 shows the dislocation vectors and fault parameters estimated for the SSE #18 (July 2006). The fault patch is ~100 km away from the axis of the Ryukyu Trench and lie on the surface of the Philippine Sea Plate slab.

The 38 SSEs possess similar horizontal dislocation vectors, but some of them showed slightly different patterns (Figure S3). Following Heki and Kataoka (2008), we assumed two longer fault geometries for SSEs, such as nos. 1, 2, and 10. The numbers of SSEs of the three different fault lengths, that is, long (~160 km in length), middle (~110 km), and short (~90 km), were 6, 10, and 22, respectively.

Heki and Kataoka (2008) demonstrated that the recurrences of these SSEs were time predictable; that is, the lower right corners of the slip accumulation diagram align (although this is not highly significant owing to the small variations of recurrence intervals). With the present data set of 38 SSEs, such time predictability seems to hold. To confirm this, we compared the correlations between slips and recurrence intervals following or preceding the events, as done by Heki and Kataoka (2008). The correlation coefficients (0.57 and 0.38) indicate that the slips have a stronger correction with the intervals after the events; that is, time-predictable recurrence is more likely. Apart from this, the slip accumulation rate (cumulative slip/lapse time) clearly varies in time (Figure 3a), and it is inadequate to fit a single line to the entire time series.

The overall rate in 1997–2016 is ~8.6 cm/yr, significantly lower than ~11 cm/yr in 1997–2007 reported by Heki and Kataoka (2008). In addition, the trends during the four periods 1997–2001, 2003–2007, 2007–2013, and 2013–2016 (slip accumulation is largely linear within these periods) are 9.3 cm/yr, 10.9 cm/yr, 6.3 cm/yr, and 10.2 cm/yr, respectively (Figure 3a). The detrended cumulative slip shown at the bottom of Figure 3a also displays two distinct increases in ~2002 and ~2013 and one gradual slowdown around 2007.

In Figure 3a, we also fit a polynomial to the lower right corners of the slip accumulation diagram. The L curve method showed that the degree-6 polynomial is the most appropriate (Figure S4). The time derivative of the polynomial is shown in Figure S5. We compare the correlation between such slopes and two quantities, that is, amount of slips (Figure 3b) and recurrence intervals (Figure 3c). It is interesting to see the stronger correlation (coefficient of 0.52) for the slips suggesting that it is increased slips rather than decreased recurrence intervals that accommodate the increase in the slip accumulation rate.

4. Mechanisms of Time-Variable Slip Accumulation

Because SSEs release accumulated strain just like regular earthquakes, stress disturbances by external forces may encourage or discourage their occurrences. Heki and Kataoka (2008) examined the possibility that static stress perturbation by EQ2–EQ4 (Figure 1b) in 2001 and 2002 might have disturbed the regular occurrence of SSEs. However, they considered it unlikely comparing the stress drop of the average SSE and the Coulomb Failure Stress change (ΔCFS) by EQ2–EQ4 at the SSE fault. Later, Nakamura (2009) considered the afterslip

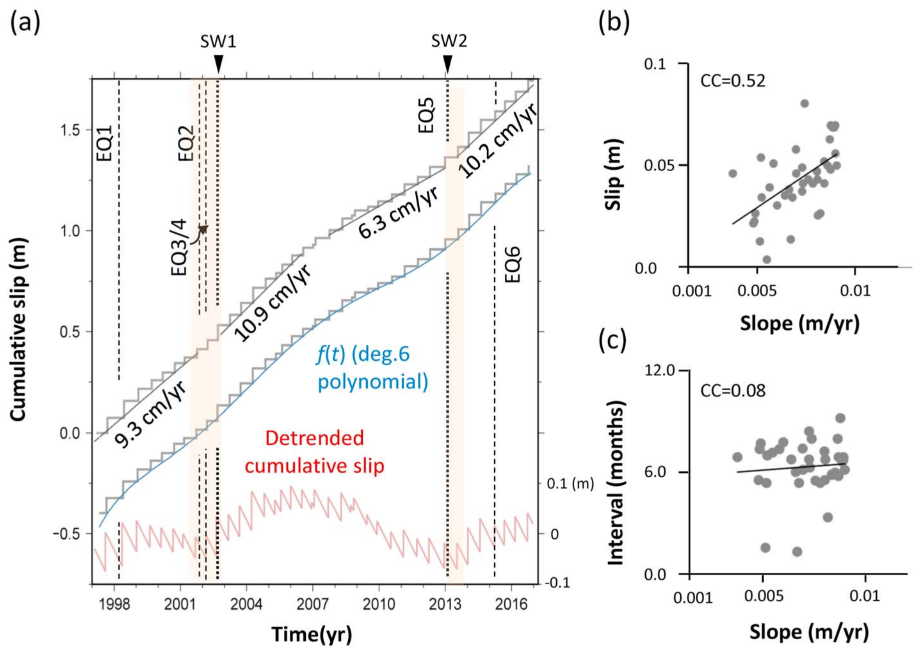

Figure 3. (a) Slip accumulation diagram of the 38 SSEs of 1997–2016. The upper diagram is fit by four lines of different trends and time periods. It is also modeled with the degree-6 polynomial, whose time derivative $f'(t)$ is shown in the Figure S5. At the bottom of the diagram, we display the detrended cumulative slip, which clearly indicates the changes. Their vertical positions are arbitrary. Dashed lines and dotted lines with triangles indicate occurrences of large earthquakes (EQ1–EQ6) and earthquake swarms (SW1–SW2), respectively. The two orange belts in the illustration represent the epochs of the slip accumulation rate increase. (b) The scatter diagram between the slips and $f'(t)$ at the SSE onset times. Its correlation coefficient is 0.52, which suggests that the two variables are positively correlated. (c) However, the correlation between the recurrence intervals and $f'(t)$ is small (correlation coefficient is 0.08).

of EQ4, that is, the 2002 March Hualien earthquake (M_w 7.1) east of Taiwan (Figure 1b), lasted for ~5 years and caused the increased slip accumulation rate.

However, no large earthquakes occurred in the neighborhood around the second increase of the slip accumulation rate in 2013. The activities of small earthquakes ($M_w > 3$) along the Ryukyu trench do not show significant changes, either (Figure 4a). Here we suggest that another mechanism might be responsible for the two increase events of the slip accumulation rate, in addition to the EQ4 afterslip (Nakamura, 2009).

Figure 4b show the seismicity within the Okinawa trough, an active back-arc spreading center located ~70 km north of the SSE patch. During the studied period, two significant earthquake swarms (SW1 and SW2) occurred, possibly the manifestation of rifting episodes at the trough axis (Nakamura & Katao, 2003). The first one was active over 2 days, 24–25 October 2002 and showed a discrete stop. The second one started on 15 April 2013 and is followed by the long duration high seismic activity at the trough. We point out that their occurrences roughly coincide with the slip accumulation rate increases in ~2002 and ~2013 (Figure 3a).

As for SW2, Ando et al. (2015) inferred the volume of the dike intrusion as ~0.4 km^3. Assuming a 2 m tensile opening of a vertical plane with the width 10 km and the length 20 km, a positive ΔCFS of ~9 kPa would have occurred at the SSE fault. This is a significant stress change amounting to ~40% of the stress drop of a SSE but does not explain the observed increase in the SSE slip accumulation rate from 6.3 cm/yr to 10.2 cm/yr lasting for years.

The Iriomote Island is located above the SSE fault patch (Figure 1b). We found that the southward motion of the GNSS station on this island accelerated from 1.4 mm/yr to 6.6 mm/yr, and from 0.8 mm/yr to 10.3 mm/yr, concurrently with SW1 and SW2, respectively (Figure 4c). Considering the long duration of the accelerated periods, we speculate that the two rifting episodes may have been followed by years of postrifting stress diffusion as seen in Iceland (e.g., Foulger et al., 1992). They would have let the block between the Okinawa Trough and the Ryukyu Trench move faster southward over several years after SW1 and SW2, and have caused the positive trend changes of the slip accumulation curve. This enhanced convergence by SW1 seems to have decayed in 5 years or so, shorter than the accelerated period lasting over a decade in NE Iceland

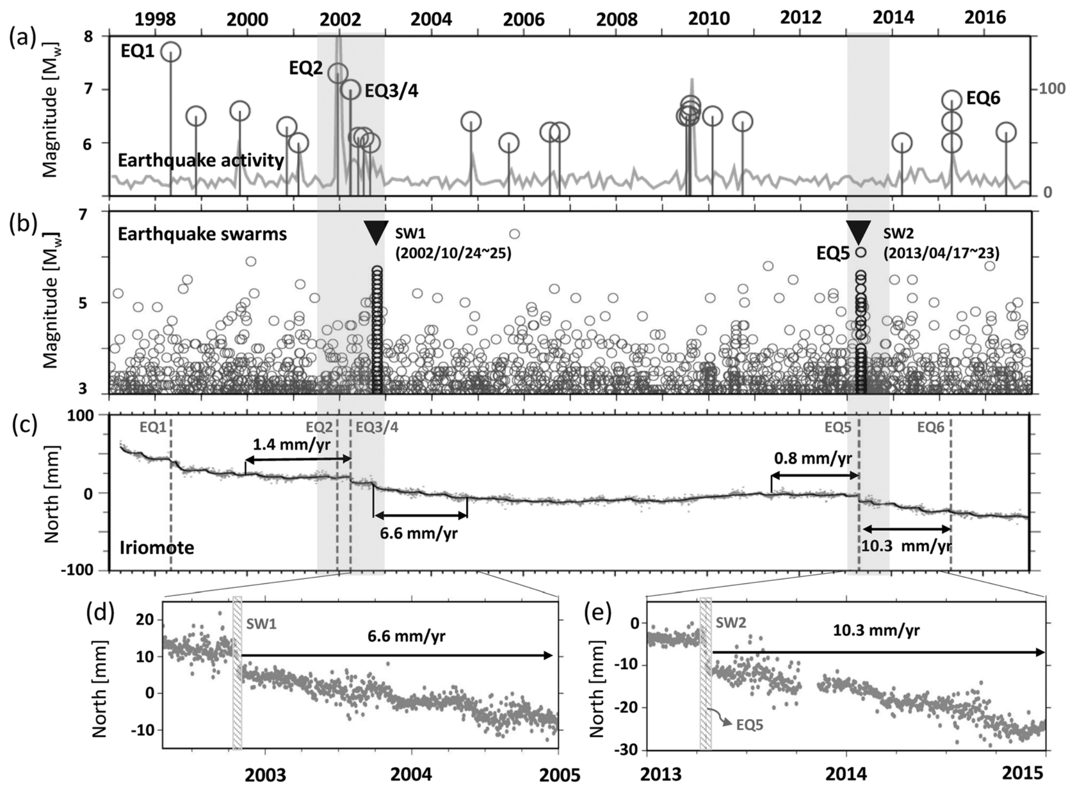

Figure 4. (a) Seismicity in the southwestern Ryukyu trench 1997–2016. Open circles indicate large earthquakes ($M_W > 6$), and the gray curve displays the number of earthquakes ($M_W > 3$), whose unit is given on the right axis. Gray shaded rectangles represent two epochs, when the slip accumulation increased. (b) Earthquake activity ($M_W > 3$) in the Okinawa trough. Two triangles indicate earthquake swarms (SW1 and SW2) in 2002 and 2013, and EQ5 (M_W 6.1) belongs to the SW2. Geometric ranges of earthquakes shown in Figures 4a and 4b are given in Figure 1b. (c) Daily north coordinate of the Iriomote station. Southward movements of this island accelerated significantly after SW1 and SW2. (d and e) The enlarge segments of Figure 4c around SW1 and SW2.

(Heki et al., 1993). The decay of the second episode is not obvious at present. As suggested by Nakamura (2009), the afterslip of EQ4 might also have contributed to the enhanced slip accumulation rate from 2002.

In general, transient stress increases in loading by external forces may enhance amount of slips and/or the event rate. For example, in the Boso area, central Japan, the transient stress increase caused by the 2011 Tohoku-Oki earthquake encouraged the earlier recurrence of the SSE (Hirose et al., 2012). However, in the southwestern Ryukyu, the transient stress increase seems to have only enhanced the amount of slips without making the recurrence intervals shorter (Figures 3b and 3c). This was contrary to our anticipation that the increased loading would be accommodated by increased event rate.

Except for two increases mentioned above, there is one gradual slowdown of the slip rate around 2007 (Figure 3a). We think this reflects the natural decay of the increase that started in 2002. Another slowdown of the slip rate would appear in the coming years, due to the decay of the second acceleration episode in 2013.

5. Conclusions

We identified 38 SSEs beneath the Iriomote Island in the southwestern Ryukyu Arc, between 1997 and 2016 at the same fault patch as studied in Heki and Kataoka (2008). There we found significant variations of the slip accumulation rate in time. The significant increase of the slip accumulation rate around 2002 and 2013 coincided with the activation of the back-arc spreading as indicated by the earthquakes swarms in the Okinawa Trough. We consider that the accelerated southward movement of the block between the Okinawa Trough and the Ryukyu Trench due to postrifting stress diffusion caused the increase of the slip accumulation rate of SSEs.

Acknowledgments

We appreciate the Editor and two reviewers who gave valuable suggestions and comments. The GNSS data used in this study are provided by GEONET of GSI Japan (http://terras.gsi.go.jp/geo_info/geonet_top.html). This work used GMT and Seis-PC software. Y. Tu was supported by the Japan-Taiwan Exchange Association (grant number of 27070).

References

Ando, M., Nakamura, M., Matsumoto, T., Furukawa, M., Tadokoro, K., & Furumoto, M. (2009). Is the Ryukyu subduction zone in Japan coupled or decoupled?—The necessity of seafloor crustal deformation observation. *Earth, Planets and Space*, *61*, 1031–1039. https://doi.org/10.1186/BF03352954

Ando, M., Ikuta, R., Tu, Y., Chen, H. Y., & Lin, C. H. (2015). The Apr 2013 earthquake swarm and dyke intrusion in the Okinawa trough, paper presented at *the Japan Geoscience Union Meeting*, Chiba, Japan, 27 May, 2015.

Beroza, C. G., & Ide, S. (2011). Slow earthquakes and nonvolcanic tremor. *Annual Review of Earth and Planetary Sciences*, *39*, 271–296. https://doi.org/10.1146/annurev-earth-040809-152531

Foulger, G. R., Jahn, C.-H., Seeber, G., Einarsson, P., Julian, B. R., & Heki, K. (1992). Post-rifting stress relaxation at the divergent plate boundary in Northeast Iceland. *Nature*, *358*, 488–490. https://doi.org/10.1038/358488a0

Heki, K., Foulger, G. R., Julian, B. R., & Jahn, C.-H. (1993). Plate dynamics near divergent boundaries: geophysical implications of postrifting crustal deformation in NE Iceland. *Journal of Geophysical Research*, *98*, 14,279–14,297. https://doi.org/10.1029/93JB00781

Heki, K., & Kataoka, T. (2008). On the biannually repeating slow-slip events at the Ryukyu Trench, southwestern Japan. *Journal of Geophysical Research*, *113*, B11402. https://doi.org/10.1029/2008JB005739

Hirose, H., Kimura, H., Enescu, B., & Aoi, S. (2012). Recurrent slow slip event likely hastened by the 2011 Tohoku earthquake. *Proceedings of the National Academy of Sciences of the United States of America*, *109*, 15,157–15,161. https://doi.org/10.1073/pnas.1202709109

Nakagawa, H., Toyofuku, T., Kotani, K., Miyahara, B., Iwashita, C., Kawamoto, S., … Sugawara, Y. (2009). Development and validation of GEONET new analysis strategy [in Japanese]. *Journal of Geography Survey Institute*, *118*, 1–8.

Nakamura, M. (2009). Aseismic crustal movement in southern Ryukyu Trench, southwest Japan. *Geophysical Research Letters*, *36*, L20312. https://doi.org/10.1029/2009GL040357

Nakamura, M., & Katao, H. (2003). Microearthquakes and faulting in the southern Okinawa Trough. *Tectonophysics*, *372*, 167–177. https://doi.org/10.1016/S0040-1951(03)00277-4

Nishimura, T. (2014). Short-term slow slip events along the Ryukyu Trench, southwestern Japan, observed by continuous GNSS. *Progress in Earth and Planetary Science*, *1*, 22. https://doi.org/10.1186/s40645-014-0022-5

Obara, K., & Kato, A. (2016). Connecting slow earthquakes to huge earthquakes. *Science*, *353*, 253–257. https://doi.org/10.1126/science.aaf1512

Okada, Y. (1992). Internal deformation due to shear and tensile faults in a half-space. *Bulletin of the Seismological Society of America*, *82*, 1018–1040.

Ozawa, S. (2014). Shortening of recurrence interval of Boso slow slip events in Japan. *Geophysical Research Letters*, *41*, 2762–2768. https://doi.org/10.1002/2014GL060072

Ozawa, S. (2017). Long-term slow slip events along the Nankai trough subduction zone after the 2011 Tohoku earthquake in Japan. *Earth, Planets and Space*, *69*, 56. https://doi.org/10.1186/s40623-017-0640-4

Rogers, G., & Dragert, H. (2003). Episodic Tremor and Slip on the Cascadia Subduction Zone: The Chatter of Silent Slip. *Science*, *300*, 1942–1943. https://doi.org/10.1126/science.1084783

Scholz, C. H., & Campos, J. (2012). The seismic coupling of subduction zones revisited. *Journal of Geophysical Research*, *117*, B05310. https://doi.org/10.1029/2011JB009003

Szeliga, W., Melbourne, T., Santillan, M., & Miller, M. (2008). GPS constraints on 34 slow slip events within the Cascadia subduction zone, 1997–2005. *Journal of Geophysical Research*, *113*, B04404. https://doi.org/10.1029/2007JB004948

Uyeda, S., & Kanamori, H. (1979). Back-Arc Opening and the Mode of Subduction. *Journal of Geophysical Research*, *84*, 1049–1061. https://doi.org/10.1029/JB084iB03p01049

Vergnolle, M., Walpersdorf, A., Kostoglodov, V., Tregoning, P., Santiago, J. A., Cotte, N., & Franco, S. I. (2010). Slow slip events in Mexico revised from the processing of 11 year GPS observations. *Geophysical Research Letters*, *115*, B08403. https://doi.org/10.1029/2009JB006852

Wallace, L. M., Webb, S. C., Ito, Y., Mochizuki, K., Hino, R., Henrys, S., … Sheehan, A. F. (2016). Slow slip near the trench at the Hikurangi subduction zone, New Zealand. *Science*, *352*, 701–704. https://doi.org/10.1126/science.aaf2349